ORIGINAL ARTICLE

Evaluating pasture cover density mapping: a comparative analysis of Sentinel-2 and Spot-5 multispectral sensor images

Taha Mansouri[1] · Javad Varvani[2] · Hamid Toranjzar[3] · Nourollah Abdi[3] · Abbas Ahmadi[4]

Abstract

Vegetation density extraction is influenced by the characteristics of satellite images, vegetation type, classification algorithm, and region, but there is little information about multispectral imaging (MSI). Studying the compatibility of the information content of sensors to replace sensors in areas where there is no easy access to their data is necessary for remote sensing (RS) studies. This study aims to assess the suitability of MSI from Sentinel-2 and Spot-5 satellites for generating pasture density maps. The Middle Kashkan watershed in the Lorestan Province of Iran was the study area. Geometric correction of the images was performed using ground control points (GCP) and the area's digital elevation model, achieving an accuracy of 0.21 pixels or better. Supervised classification techniques including parallelogram, minimal distance, maximum likelihood, and artificial neural network (ANN) algorithms were applied to the primary MSI of each satellite, as well as the integrated image of Spot-5 and the resulting pasture density map. Three density categories were considered: 5–25%, 25–50%, and over 50%. To validate the accuracy of the classification, a ground truth map of the region was created by interpreting a referenced official digital orthophotomosaic image at a scale of 1:40,000. Comparative analysis of the classified images revealed that the Sentinel-2 image with PCA-2-8 band composition and ANN classification algorithm yielded superior results, with an overall accuracy of 65.72% and a kappa coefficient of 0.08, compared to the Spot-5 image with PCA-3-1 band composition and the ANN classification algorithm. Spot-5 satellite images demonstrated greater effectiveness in generating pasture cover maps across the three density categories. These findings suggest that satellite images with suitable spatial and spectral resolution can be effectively utilized for generating accurate pasture density maps and monitoring long-term pasture preservation, particularly in regions characterized by high aerial photography altitudes in pasture areas. This approach holds the potential for effective pasture management and conservation efforts on a global scale.

Keywords Supervised classification · Multispectral imaging · Band composition · Sentinel-2 · Spot-5 · Overall accuracy · Kappa coefficient

Introduction

With the rapid development of the population, as well as the destruction and limitation of resources, it is now necessary to understand the various aspects of the natural environment to apply scientific management (Zahoor et al. 2022). In addition to saving research time, the continuous, fast, and precise depiction of resources has made it possible to analyze the level of change and correct planning for restoring and managing devastated areas (Krichen et al. 2023). Based on this, pasture maps can be created in various ways, including ground mapping, aerial photo interpretation, and satellite image interpretation. In the meantime, satellite images are widely recognized as essential data sources for producing vegetation and pasture maps (Thanh Noi and Kappas 2017).

✉ Javad Varvani
drjavadvarvani@gmail.com

1 Department of Agriculture and Natural Resources, Arak Branch, Islamic Azad University, Arak, Iran

2 Department of Natural Resources and Environmental Sciences, Applied Plant Science Research Center, Arak Branch, Islamic Azad University, Arak, Iran

3 Department of Environment, Faculty of Agriculture and Natural Resources, Arak Branch, Islamic Azad University, Arak, Iran

4 Food Security Research Centre, Arak Branch, Islamic Azad University, Arak, Iran

It is costly and time-consuming to collect data from expansive pastures using traditional methods. Using conventional methods to collect data from expansive pastures is expensive and time-consuming (Dastgheyb Shirazi et al. 2021a, b). Although aerial image mosaics produce highly accurate maps, the process is lengthy. Therefore, it is essential to employ simple and inexpensive procedures based on the region's characteristics and the type of information desired (Phiri et al. 2020). In such circumstances, satellite images are a viable option. Due to benefits like multi-spectrally, imaging in extremely short periods, and availability, satellite images have made it feasible to extract information in the shortest time possible and monitor the change process (Alvarez-Hess et al. 2021). There is a long history of using satellite images to extract vegetation data and create maps. However, one limitation of some MSI is their lack of spatial resolution, making it difficult for the RS community to process land use and land cover maps accurately and quickly (Gómez et al. 2016).

As a result, given the availability of MSI, selecting the right image can reduce the cost of making national maps and improve the precision of provided statistics (Li et al. 2021). In addition, it is possible to develop thematic maps for pasture studies, such as the map of pasture density and the map of restored regions, and to use RS methods and images to assess changes over time (Oliveira et al. 2020).

The Sentinel-2 satellite is the latest generation of earth observation satellites belonging to the European Space Agency, which is mainly designed to monitor resources in land and coastal areas (Drusch et al. 2012). This satellite was launched in 2015 and compared to the Landsat series of satellites, it has better spatial, spectral, and temporal resolution. This satellite has made it effective in different applications such as forest classification and product monitoring, detecting built-up areas, and water environment monitoring (Immitzer et al. 2016; Lefebvre et al. 2016; Paul et al. 2016; Pesaresi et al. 2016). The most important limitation of using this data in monitoring the phenomena is the short period of activity of this satellite as well as the limitations related to obtaining data in cloudy conditions (Vajsová et al. 2020). As a result, in long-term monitoring using time series, it is necessary to use the images of other sensors that have the most matching information content with Sentinel-2 images. The long-term and free archive of Landsat images is the best option to check this match (Crawford et al. 2023). The data from two sensors have made it possible to investigate visits of less than 5 days for a specific area with moderate spatial resolution (Bannari 2019). As a result, the simultaneous use of these two meters provides the possibility of monitoring resources in short time intervals.

Comparing the data content of different sensors to replace them in cases where it is not possible to access any of the sensors has been investigated in many researches (Korhonen et al. 2017; Zhang et al. 2018). This lack of access can include the restrictions applied to users of some countries or the existence of unfavorable weather conditions for taking satellite images. In this situation, alternative gauge data can be used. Zhang et al. (2018) investigated the effect of atmospheric correction on spectral indices extracted from Sentinel-2 sensors and Landsat 8 images. The findings of this study showed that the normalized vegetation index (NDVI) extracted from Sentinel-2 and Landsat 8 data does not have statistically significant differences with each other and that the NDVI values of one gauge can be used instead of the NDVI index of another gauge if necessary. In another study, the area index made from the MSI of these two satellites was extracted and compared with each other (Xi et al. 2019). The researchers concluded that the Sentinel-2 sensor has a better performance for extracting built-up areas (Feng et al. 2021). This superiority is more apparent when using spectral indices in the classification process. The Landsat image showed the area of built-up areas more than the validation data (Xie et al. 2020).

A review of the literature shows that, in general, in most studies, there is a good match between the corresponding bands in Iran of the MSI of these two satellites (Forouzan & Arfania 2020). Despite the extensive use of Sentinel-2 data, no specific research has been done to check the information content of the Sentinel-2 MSI sensor and Landsat 8 OLI. Most previous research has investigated other types of sensors. Alavipanah et al. (2006) compared the correlation of bands thematic mapper (TM) and enhanced thematic mapper (ETM$^+$) in two desert areas and an urban area located in the semiarid region of Damghan. The results showed that in both regions, the correlation between the thermal band and reflective bands between the two sensors is low, so they do not contain duplicate information. Also, numerous scholars have investigated vegetation cover using satellite images and concluded that this technique is appropriate for investigating the dynamics of pasture vegetation (Malinowski et al. 2020). Huong et al. (2017) extracted eleven classifications from Sentinel-2 images in the Dak Nong area of Vietnam and applied them to create a map of the land use and vegetation in various seasons using four classification methods. Overall accuracy for all seasons and classification methods ranged between 63.9 and 80.3%, while the kappa coefficient was between 0.611 and 0.80. Several studies demonstrate that the characteristics of satellite images, the type of vegetation, the classification algorithm, and the examined area all significantly impact the extraction of vegetation density. Rudiastari et al. (2018) utilized Spot-6 data to generate a biomass map of mangrove forests in Indonesia's East Lembak. They concluded that estimating the amount of biomass in the mangrove forest is necessary for determining how productive and sustainable it is, as well as how much

carbon can be released as carbon dioxide during deforestation. Abdi (2020) created the South Sudan land use map using Sentinel-2 satellite imagery and nonparametric classification methods. The findings revealed that the support vector machine method performed much better in extracting the land use map, with an overall accuracy of 75.8%. Tawab and Fantan (2020) assessed land use changes in the north-western areas using Landsat TM satellite imagery and supervised classification. The results indicated that the kappa coefficient for the land use map in 1986, 2002, and 2018 was correspondingly 0.79, 0.83, and 0.89.

Considering the free access to the archive of the Landsat satellite series and the Sentinel-2 data, it seems necessary to check the compatibility of the information content of these two sensors. In case of acceptable compliance, it is possible to use the combined images of these two satellites in a long-term time series with medium spatial resolution. To the best of our knowledge, few previous studies have used Sentinel-2 and Spot-5 MSIs to create a density map of pasture cover. For this purpose, the current research aimed to compare Sentinel-2 and Spot-5 MSIs to create a density map of pasture cover in the middle Kashkan drainage basin in Lorestan Province, Iran. To do this, in the first part, the correlation of the corresponding bands of the two sensors was investigated. Then, the effectiveness of these two sensors in classifying the land cover in a heterogeneous area has been measured. An ANN algorithm was used for classification, and finally, the results were validated using existing maps and satellite images with high resolution. Therefore, the major innovation of this study lies in the integration of high-resolution Sentinel-2 data and Spot-5 MSIs and an ANN algorithm for creating a density map of pasture cover at a fine scale.

Materials and methods

Study area

The study area is 33,196 ha in western Iran, with a longitude of 48° to 48° 07′ 30″ and latitude of 33° 45′ to 33° 52′ 30″. The area's highest and lowest elevations are 3639 and 1812 m above sea level, respectively. The maximum annual precipitation in the region is 1212 mm, while the lowest is 53 mm (Azadi et al. 2020) (Fig. 1).

Methodology

Sentinel-2 satellite images from 2018, with a polar orbit and 13 spectral bands in the visible, near-infrared, and short-infrared ranges, were used in this study. In terms of spatial resolution, these bands fall into three groups. Bands 2, 3, 4, and 8 have a spatial resolution of 10 m, whereas bands 5, 6, 7, 11, and 12 have a spatial resolution of 20 m. Bands 1 and 9 have a spatial resolution of 60 m. In addition, the Spot-5 satellite's HRG sensor data from 2018, which involves four MSI bands (green, red, near-infrared, and mid-infrared) with a spatial resolution of 10 m, was utilized. Two sheets of the area's 1:25,000-scale topographic map were used to recognize and explore the area and assist in creating the ground truth map. Figure 2 shows the flowchart of the study implementation process.

Quality assessment of satellite data

Before using satellite data for digital analysis and geometric correction, the data's geometric and radiometric errors were evaluated for accuracy. No anomalies were found while
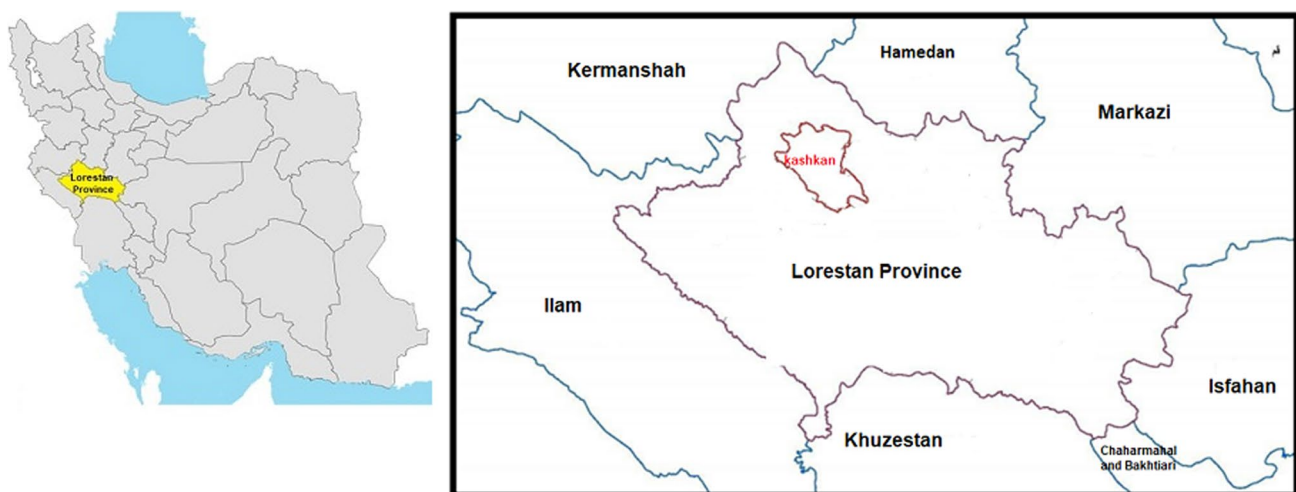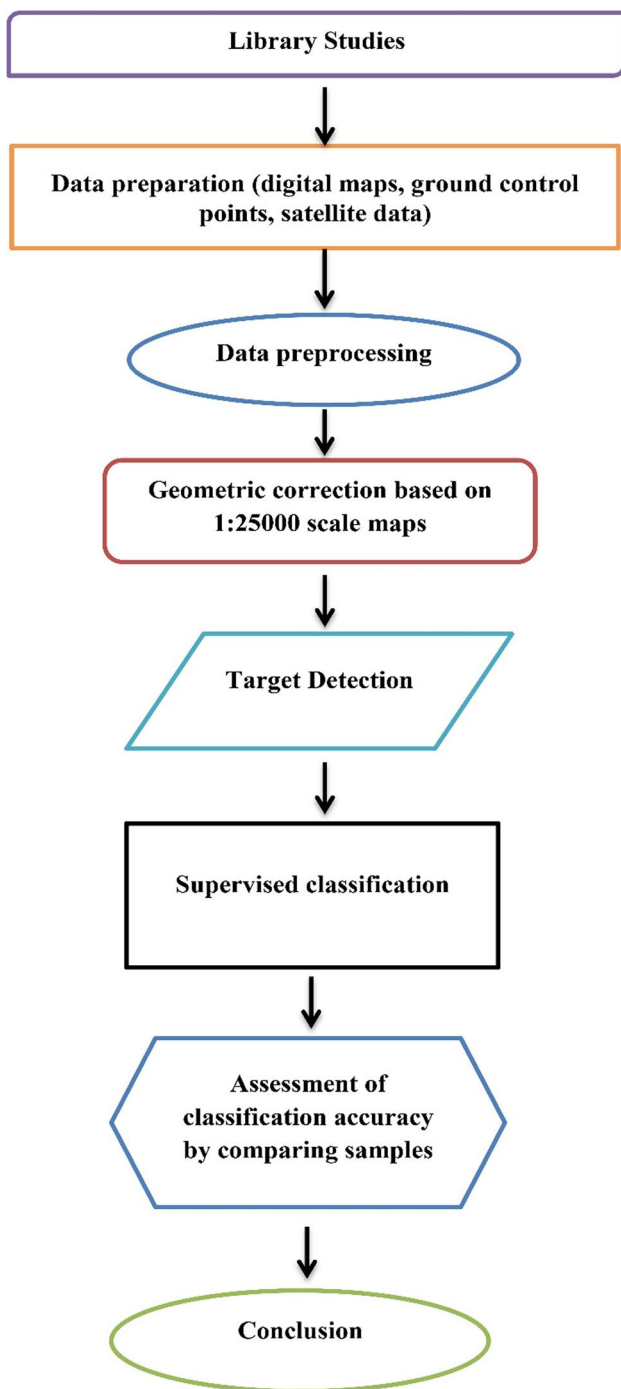

Fig. 1 Location of the study area

Library Studies

↓

Data preparation (digital maps, ground control points, satellite data)

↓

Data preprocessing

↓

Geometric correction based on 1:25000 scale maps

↓

Target Detection

↓

Supervised classification

↓

Assessment of classification accuracy by comparing samples

↓

Conclusion

Fig. 2 Flowchart of study implementation process

analyzing the radiometric quality of the satellite data for errors such as striping, line drop-outs, and duplicate pixels using image magnification and checking histograms and related statistics. The satellite data were georeferenced with the ground truth map via nonparametric geometric matching of the images, using maps and GCPs. Fifty-five GCPs were selected from the 1:25,000 digital topographic map

of the region for this purpose, and geometric matching was performed using the first-order equation with an RMSE of 0.21 pixels. The nearest neighbor method was used for resampling. The geometric correction was done well by stacking the line features on the images.

Principal component analysis (PCA)

Given the ability to apply multiple processes to satellite images as well as the original data during the data analysis process, several processing methods, such as principal component analysis, have been applied to the data of both sensors. In this technique, the statistical properties of several bands are employed to evaluate data into its primary components. This method generates new images based on the number of available bands and the degree of correlation between bands. The first band contains the most information, the highest standard deviation, and the highest variance; these values decrease with each succeeding band. After creating the available images using the principal component analysis, the first band with the most information was used to prepare the optimal band combination and classify the images.

Classification and preparation of pasture density map

The necessary procedures were carried out on the color image after selecting the trained samples required for the classification of pasture density in the area, following the region's knowledge and using the collected secondary information. Satellite images were classified using the appropriate band set and the parallelogram, minimum distance, maximum likelihood, and ANN algorithms.

Ground truth map

To verify the classification accuracy of satellite data, a ground truth map is required for comparison purposes. The cluster-systematic sampling method was used to generate the ground truth map for this study. At the intersection of UTM lines and 1:25,000 maps, a basic grid with dimensions of 1000 m by 1000 m was created for this method. From this grid, 117 samples were collected, and the GPS coordinates of the sample centers were recorded in two directions. In each plot, north–south and east–west samples were collected. In addition, the percentage of pasture covering in each sample plot was calculated based on the sample plot's area, and according to the Natural Resources and Watershed Management Organization of Iran's standard, it was categorized into three density classes: 5%–25%, 25%–50%, and more than 50%.

Accuracy assessment

To assess the accuracy, the results of the digital categorization of satellite images were compared to the ground truth map and control points, and error value evaluation tables were created. The accuracy was examined using criteria for overall accuracy and the kappa coefficient.

Overall accuracy This accuracy gives the overall results of the confusion matrix. It is calculated by dividing the total number of correct pixels (diagonal values) by the total number of pixels in the confusion matrix. On the other hand, accuracy levels that are accepted by users may not be acceptable by other users for a certain task (Geremew 2013).

Kappa coefficient (KC) The kappa statistic was used to measure the agreement between two sets of categorizations of a dataset (Table 1) and used to estimate the accuracy of predictive models by measuring the agreement between the predictive model and a set of field-surveyed sample points (Moriasi et al. 2007).

Results and discussion

Ground truth map

The ground truth map was created in three pasture classes: 5–25%, 25–50%, and more than 50% using 1:25,000 maps, GCPs, and knowledge of the local environment (Fig. 3). Pakkhesal and Bonyad (2013) investigated the classification of Caspian forests' canopy densities using data from Landsat

Table 1 Kappa coefficient classification

Number	Kappa coefficient	Rate
1	Less than 0.4	Poor
2	$0.4 < KC < 0.5$	Fair
3	$0.55 < KC < 0.7$	Good
4	$0.7 < KC < 0.85$	Very Good
5	$KC > 0.85$	Excellent
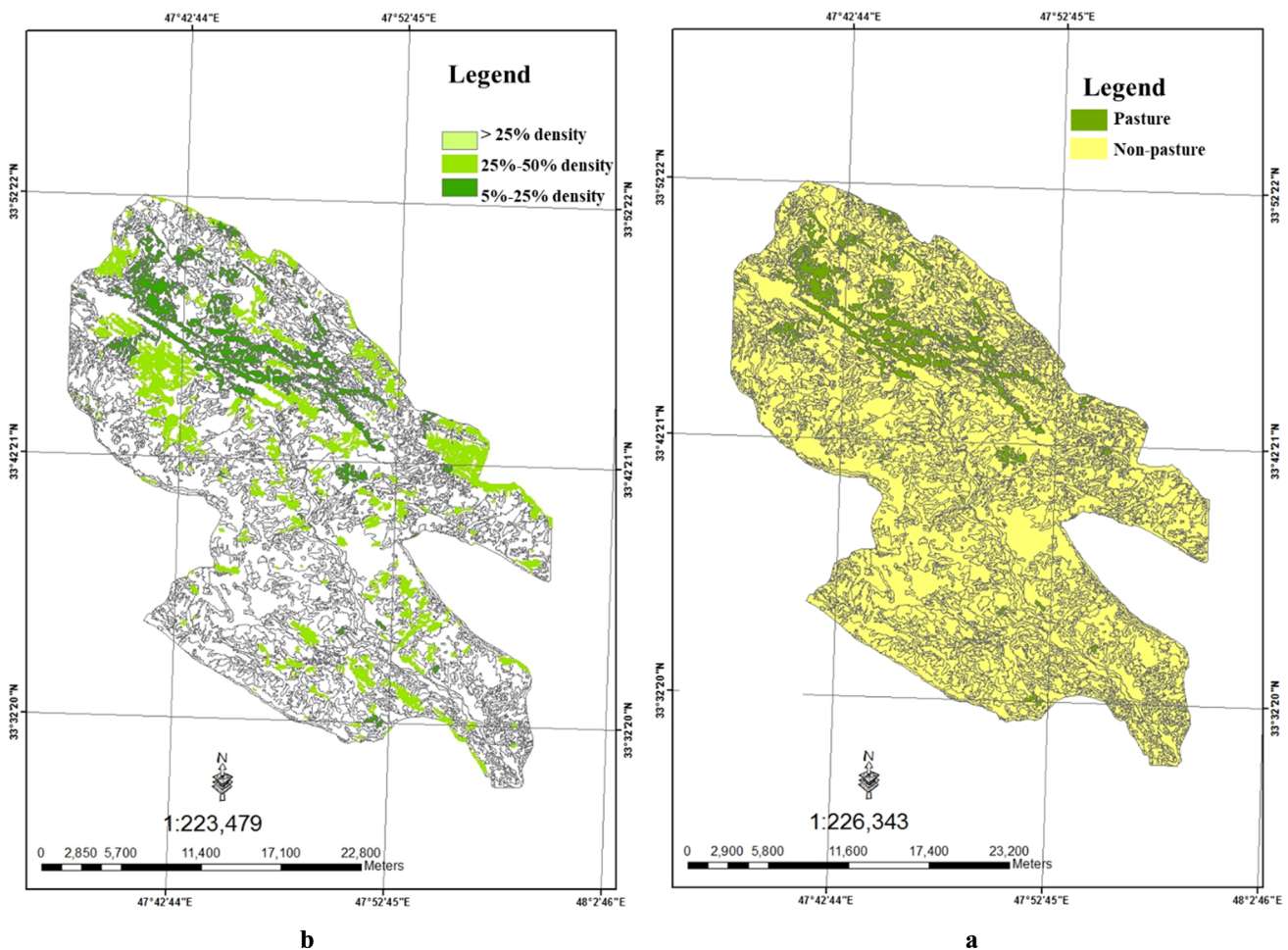
Fig. 3 Map of pasture covering (**a**) and pasture areas in three density classes (**b**)

ETM + sensors. The map of canopy density was produced in the categories of 5%–25%, 25%–50%, 50%–75%, 75%-100%, and one layer without forest. The optimal index factor method was used to determine the optimal band combination. The five images of Sentinel-2 and Spot-5 were produced by combining the four primary bands and the first band derived from the data analysis of principal component analysis.

The optimal band composition for Sentinel-2 is thus 8-4-2. With the PCA band applied, the optimal combination would be 8-4-PCA. The best possible band combination for Spot-5 is 1-4-2-1, while the optimal band combination for PCA is 1-2-PCA. This research showed that it is possible to distinguish between pasture and agricultural areas on aerial photographs of the area and also on existing images. Furthermore, in the preparation of the ground reality map, the interpretation of aerial photographs alone is not enough, and other auxiliary elements should be used in the map production process. Among these elements used are existing maps, field control, and familiarity with the situation of the region. Finally, the ground reality map was prepared in the form of a map of pasture and non-pasture areas, as well as three classes of pasture in the target area.

Satellite image classification

Using Sentinel-2 and Spot-5 images, the classification map of pasture areas into three density classes (pasture with a density of 5–25%, 25–50%, and more than 50%) was created after selecting the best appropriate combination of bands and classification algorithms (Fig. 4). The varying spectral range of the bands, the spectral interference of the image bands, the variation in the statistical characteristics of the numerical values of the samples in the images, and the classification methods can all affect the resolution of the classes in various images (Sekovski et al. 2014).

The most accurate ANN classification map in the Sentinel-2 image had a PCA-2-8 band composition, an overall accuracy of 65.72%, and a kappa coefficient of 0.08. Meanwhile, the ANN classification map with 3-1-PCA band composition an overall accuracy of 70.53% and a kappa coefficient of 0.65 had the highest accuracy in the Spot-5 image. Based on the classification of Moriasi et al. 2007), the Sentinel-2 and Spot-5 spot images are classified as poor and good respectively (Table 2).

Bazrafkan et al. (2014) used parallelogram classification methods, minimum distance from the mean, maximum

Fig. 4 Classification of pasture areas into three density classes A: Sentinel-2 image and B: Spot-5
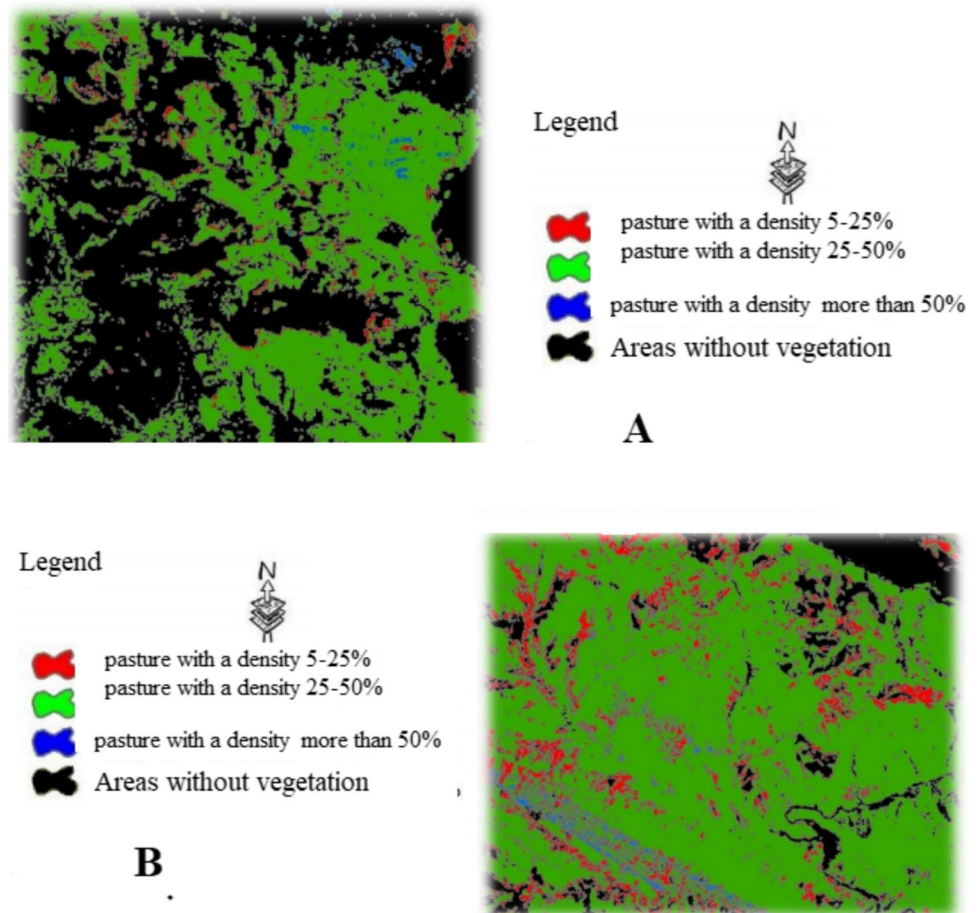
Table 2 Accuracy estimation results of different classification algorithms in Sentinel-2 and Spot-5 images

ANN		Maximum likelihood		Minimum distance		Parallel		Images
Kappa coefficient	Overall accuracy (%)	Kappa coefficient	Overall accuracy (%)	Kappa coefficient	Overall accuracy (%)	Kappa coefficient	Overall accuracy (%)	
0.08	65.72	0.06	36.82	− 0.18	21.22	0.06	51.18	Sentinel-2
0.65	70.53	0.1	51.82	0.08	50.32	-0.02	60.85	Spot-5

Table 3 Comparison of the results obtained in the classification of pasture into three density classes and the use of filter

Kappa coefficient	Overall accuracy (%)	Image classification
0.1	67.35	Sentinel-2 using 3×3 filter majority
0.23	71.61	Spot-5 using 3×3 filter majority

likelihood, and an ANN to construct a canopy density map of Zagros forests. With three density classes (thin, semi-dense, and dense), the ANN method produced the highest overall accuracy and kappa coefficient of 78.47% and 0.66%, respectively. Hu et al. (2018) created a vegetation map of Qingdao, China, using Landsat 8 satellite images and an ANN classification algorithm. According to the findings, the classified map's overall accuracy is 82%, and its kappa coefficient is 0.76. Furthermore, compared to the maximum likelihood and support vector machine algorithms, the authors claimed that the ANN's overall classification accuracy increased by 5 and 14%, respectively.

The pasture cover map created using the satellite mentioned above image in the form of three density classes has improved accuracy, as shown in Table 1, overall accuracy (70.53), and kappa coefficient (0.65) of the ANN classification method in the Spot-5 image. The extent of each pasture density class is as follows: The second class has a density of 25–50% with an area of 22,962 hectares > the first class has a density of 5–25% with an area of 9804 hectares > the third class has a density of more than 50% with an area of 430 hectares. According to this information, the most considerable portion of the research area contains a pasture density that ranges from 25 to 50%.

Many organizations, such as the Natural Resources and Watershed Management Organization, must adopt effective measures with the aid of other decision-making authorities to protect and restore pastures and prevent the degradation of these valuable ecosystems (Motamedi et al. 2020; Feng et al. 2021; Krichen et al. 2023). Using the filter command, a comparison was performed following the completion of the classification to achieve superior results. A 3×3 filter with the average method was used to classify the image of Sentinel-2 and Spot-5 within the specified range (Table 3). Based on the data, it appears that the classified images from

the Spot-5 satellite contain a higher number of pure pixels than the images from the Sentinel-2 satellite.

Using MSI for accurate pasture density maps offers several advantages, including enhanced spectral information, improved spatial resolution, temporal coverage, and wide coverage and accessibility. MSI captures data across multiple wavelengths, allowing for a more comprehensive understanding of vegetation characteristics and density. This enables better discrimination and classification of pasture areas (Forouzan & Arfania 2020; Oliveira et al. 2020; Li et al. 2021; De Luca et al. 2022; Ku et al. 2023). MSI from satellites like Sentinel-2 and Spot-5 typically provide high-resolution imagery, allowing for the detection of built-up areas of fine-scale variations in pasture density (Rudiastuti et al. 2018; Xie et al. 2020; Kearney et al. 2022). This level of detail aids in accurate mapping and monitoring of pasture areas. Furthermore, satellites capture MSI repeatedly over time, providing a temporal dimension to the analysis (Ku et al. 2023). This enables the monitoring of changes in pasture density over seasons, years, or even longer periods, facilitating long-term pasture management and conservation efforts. Finally, satellite imagery covers large areas, making it suitable for regional- or global-scale analyses (Vajsová et al. 2020; De Luca et al. 2022; Sangjan et al. 2022; Crawford et al. 2023). Additionally, MSI is often publicly accessible or available for purchase, allowing researchers and land managers to access the data easily.

Conclusion

The pasture coverage density map for Lorestan province (middle Kashkan drainage basin) was created by comparing images from Sentinel-2 and Spot-5 MSI sensors. Compared to other algorithms, it was discovered that the ANN classification algorithm has the highest accuracy in both images. The overall accuracy (70.53) and kappa coefficient (0.65) of the ANN classification algorithm in the Spot-5 image show that this satellite image is more reliable for producing the map of pasture cover in three density classes. For pasture density classification, Spot-5 images surpass Sentinel-2 because spectral capability is more effective than spatial resolution. Most of the study area has pasture cover ranging from 25 to 50%. Therefore, it can be concluded that

only using and referring to the overall accuracy to evaluate the capability of satellite images in examining the process of changes cannot be enough. Rather, other criteria such as the kappa coefficient should be used for this purpose. The higher the kappa coefficient is, the more accurately the location and amount of the pasture have been determined into three density classes. The pasture density classification map is an important management tool for managing pasture use, reducing stress on pastures, and preventing their devastation. Furthermore, because of its broad coverage and quick access to satellite images, this tool can produce maps of vegetation and pastures and assess, control, and monitor pastures over a specific period. According to the results, the combined use of Sentinel-2 and Spot-5 sensor data can be very suitable in preparing a map of pasture and non-pasture areas as well as classifying pasture areas into three density classes. It is suggested that the Spot-5 satellite images be used to prepare and update pasture coverage maps in the western part of Iran on a scale of 1:25,000 due to the appropriate and high accuracy obtained compared to the Sentinel-2 sensor. Also, it is recommended to use Spot-5 sensor images in different periods in the growing season to compare the surface of pasture areas in the west of Iran. To the best of our knowledge, this work is one of the attempts to integrate Sentinel-2 and Spot-5 MSIs to create a density map of pasture cover in the world.

Author contributions Taha Mansouri contributed to writing—original draft, investigation, Methodology; Javad Varvani contributed to supervision, conceptualization, project administration, funding acquisition; Hamid Toranjzar contributed to supervision; Nourollah Abdi and Abbas Ahmadi contributed to advising;.

Data availability The data used to support the findings of this study are available from the corresponding author upon request.

Declarations

Conflict of interest No conflict of interest has been stated by the authors of the article.

Informed consent Informed consent was obtained from all individual participants included in the present study.

References

Abdi AM (2020) Land cover and land use classification performance of machine learning algorithms in a boreal landscape using Sentinel-2 data. Gisci Remote Sens 57(1):1–20

Alavipanah SK, Ehsani AH, Matinfar H, Rafiei A, Amiri A (2006) Comparison of information of TM and ETM+ bands in arid and urban areas. Geogr Res 56:47

Alvarez-Hess PS, Thomson AL, Karunaratne SB, Douglas ML, Wright MM, Heard JW, Jacobs JL, Morse-McNabb EM, Wales WJ, Auldist MJ (2021) Using multispectral data from an unmanned aerial system to estimate pasture depletion during grazing. Anim Feed Sci Technol 275:114880

Azadi F, Sadough SH, Ghahroudi M, Shahabi H (2020) Zoning of flood risk in Kashkan River basin using two models WOE and EBF. J Geogr Environ Hazards 9(1):45–60. https://doi.org/10.22067/geo.v9i1.83090

Bannari A (2019) Synergy between Sentinel-MSI and Landsat-OLI to support high temporal frequency for soil salinity monitoring in an arid landscape. Research Developments in Saline Agriculture. Springer, Singapore, pp 67–93

Bazrafkan A, Bavaghar MP, Fathi P (2014) Capability of Liss III data for forest canopy density mapping in Zagros forests (Case study: Marivan Forests). Iran J for 6(4):387–401

Crawford CJ, Roy DP, Arab S, Barnes C, Vermote E, Hulley G, Zahn S (2023) The 50-year Landsat collection 2 archive. Sci Remote Sen 8:100103. https://doi.org/10.1016/j.srs.2023.100103

DastgheybShirazi SS, Ahmadi A, Abdi N, Toranj H, Khaleghi MR (2021) Investigation of the effect of long-term grazing exclosure on the soils physicochemical properties in arid and semi-arid rangelands (Case study: Bozdaghin rangelands, North Khorasan, Iran). Environ Monit Assess 193(1):51. https://doi.org/10.1007/s10661-020-08819-9

Dastgheyb Shirazi SS, Ahmadi A, Abdi N, Toranj H, Khaleghi MR (2021) Moderate grazing is the best measure to achieve the optimal conservation and soil resources utilization (Case study: Bozdaghin rangelands, North Khorasan, Iran). Environ Monit Assess 193(9):549. https://doi.org/10.1007/s10661-021-09334-1

De Luca G, Silva MN, J, Di Fazio S, Modica G, (2022) Integrated use of Sentinel-1 and Sentinel-2 data and open-source machine learning algorithms for land cover mapping in a Mediterranean region. Eur J Remote Sens 55(1):52–70

Drusch M, Del Bello U, Carlier S, Colin O, Fernandez V, Gascon F, Hoersch B, Isola C, Laberinti P, Martimort P, Meygret A (2012) Sentinel-2: ESA's optical high-resolution mission for GMES operational services. Remote Sens Environ 120:25–36

Feng X, Li P, Cheng T (2021) Detection of urban built-up area change from Sentinel-2 images using multiband temporal texture and one-class random forest. IEEE J Sel Top Appl Earth Obs Remote Sens 14:6974–6986. https://doi.org/10.1109/JSTARS.2021.3092064

Forouzan M, Arfania R (2020) Integration of the bands of ASTER, OLI, MSI remote sensing sensors for detection of hydrothermal alterations in southwestern area of the Ardestan, Isfahan Province, Central Iran. Egypt J Remote Sens Space Sci 23(2):145–157. https://doi.org/10.1016/j.ejrs.2018.10.005

Geremew AA (2013) Assessing the impacts of land use and land cover change on hydrology of watershed: a case study on Gigel-Abbay Watershed. Lake Tana Basin, Ethiopia.

Gómez C, White JC, Wulder MA (2016) Optical remotely sensed time series data for land cover classification: a review. ISPRS J Photogramm Remote Sens 116:55–72

Hu Y, Zhang Q, Zhang Y, Yan H (2018) A deep convolution neural network method for land cover mapping: a case study of Qinhuangdao. China Remote Sens 10(12):1–16

Huong NT, Tuan TA, Thach VT, Tin HC (2017) A review of seagrass studies by using satellite remote sensing data in the Southeast Asia: status and potential. Vietnam J Sci Technol 55(4C):148–154

Immitzer M, Vuolo F, Atzberger C (2016) First experience with sentinel-2 data for crop and tree species classifications in Central Europe. Remote Sens 8:166

Kearney SP, Porensky LM, Augustine DJ, Gaffney R, Derner JD (2022) Monitoring standing herbaceous biomass and thresholds in semiarid rangelands from harmonized Landsat 8 and Sentinel-2 imagery to support within-season adaptive management. Remote Sens Environ 271:112907

Korhonen L, Packalen P, Rautiainen M (2017) Comparison of Sentinel-2 and Landsat 8 in the estimation of boreal forest canopy cover and leaf area index. Remote Sens Environ 195:259–274

Krichen M, Abdalzaher MS, Elwekeil M, Fouda MM (2023) Managing natural disasters: an analysis of technological advancements, opportunities, and challenges. Internet Things Cyber-Phys Syst 4:99–109

Ku KB, Mansoor S, Han GD, Chung YS, Tuan TT (2023) Identification of new cold tolerant Zoysia grass species using high-resolution RGB and multi-spectral imaging. Sci Rep 13(1):13209

Lefebvre A, Sannier C, Corpetti T (2016) Monitoring urban areas with Sentinel-2A data: application to the update of the Copernicus high resolution layer imperviousness degree. Remote Sens 8(7):606

Li H, Zech J, Ludwig C, Fendrich S, Shapiro A, Schultz M, Zipf A (2021) Automatic mapping of national surface water with OpenStreetMap and sentinel-2 MSI data using deep learning. Int J Appl Earth Obs Geoinf 104:102571. https://doi.org/10.1016/j.jag.2021.102571

Malinowski R, Lewiński S, Rybicki M, Gromny E, Jenerowicz M, Krupiński M, Nowakowski A, Wojtkowski C, Krupiński M, Krätzschmar E, Schauer P (2020) Automated production of a land cover/use map of Europe based on Sentinel-2 imagery. Remote Sens 12(21):3523

Moriasi DN, Arnold JG, Van Liew MW, Bingner RL, Harmel RD, Veith TL (2007) Model evaluation guidelines for systematic quantification of accuracy in watershed simulations. Trans ASABE 50(3):885–900

Motamedi J, Jalili A, Arzani H, Khodagholi M (2020) Causes of rangeland degradation in the country and solutions to get out of the current situation. Iran Nat 5(4):21–44

Oliveira J, Campbell EE, Lamparelli RA, Figueiredo GK, Soares JR, Jaiswal D, Sheehan JJ (2020) Choosing pasture maps: an assessment of pasture land classification definitions and a case study of Brazil. Int J Appl Earth Obs Geoinf 93:102205. https://doi.org/10.1016/j.jag.2020.102205

Pakkhesal E, Bonyad AE (2013) Classification and delineating natural forest canopy density using FCD model (Case study: Shafarud area of Guilan). Iran J for Poplar Poplar Res 21(1):99–114

Paul F, Winsvold SH, Kääb A, Nagler T, Schwaizer G (2016) Glacier remote sensing using sentinel-2 Part II: mapping glacier extents and surface facies, and comparison to landsat 8. Remote Sen 8(7):575

Pesaresi M, Corbane C, Julea A, Florczyk AJ, Syrris V, Soille P (2016) Assessment of the added-value of sentinel-2 for detecting built-up areas. Remote Sens 8:299

Phiri D, Simwanda M, Salekin S, Nyirenda VR, Murayama Y, Ranagalage M (2020) Sentinel-2 data for land cover/use mapping: a review. Remote Sens 12(14):1–35

Rudiastuti AW, Yuwono DM, Hartini S (2018) Mangrove mapping using SPOT 6 at East Lombok Indonesia. IOP Conf Series: Environ Earth Sci 65(1):1–12

Sangjan W, Carpenter-Boggs LA, Hudson TD, Sankaran S (2022) Pasture productivity assessment under mob grazing and fertility management using satellite and uas imagery. Drones 6(9):232

Sekovski I, Stecchi F, Mancini F, Del Rio L (2014) Image classification methods applied to shoreline extraction on very high-resolution multispectral imagery. Inter J Remote Sens 35(10):3556–3578

Tewabe D, Fentahun T (2020) Assessing land use and land cover change detection using remote sensing in the Lake Tana Basin. Northwest Ethiopia Cogent Environ Sci 6:1778998

Thanh Noi P, Kappas M (2017) Comparison of random forest, k-nearest neighbor, and support vector machine classifiers for land cover classification using Sentinel-2 imagery. Sensors 18(1):1–18

Vajsová B, Fasbender D, Wirnhardt C, Lemajic S, Devos W (2020) Assessing spatial limits of sentinel-2 data on arable crops in the context of checks by monitoring. Remote Sens 12(14):2195. https://doi.org/10.3390/rs12142195

Xi Y, Thinh NX, Li C (2019) Preliminary comparative assessment of various spectral indices for built-up land derived from Landsat-8 OLI and Sentinel-2A MSI imageries. Europ J Remote Sens 52(1):240–252

Xie Z, Han Y, Sun L, Ping J (2020) Analysis of land cover evolution within the built-up areas of provincial capital cities in northeastern China based on nighttime light data and Landsat data. PLoS ONE 15(10):e0239371. https://doi.org/10.1371/journal.pone.0239371

Zahoor Z, Latif MI, Khan I, Hou F (2022) Abundance of natural resources and environmental sustainability: the roles of manufacturing value-added, urbanization, and permanent cropland. Environ Sci Pollut Res 29(54):82365–82378

Zhang HK, Roy DP, Yan L, Li Z, Huang H, Vermote E, Roger JC (2018) Characterization of Sentinel-2A and Landsat-8 top of atmosphere, surface, and nadir BRDF adjusted reflectance and NDVI differences. Remote Sens Environ 215:482–494